

<https://doi.org/10.48047/AFJBS.6.7.2024.2617-2663>



## **FORMULATION AND EVALUATION OF PEO LOADED NANO FIBROUS IN SITU GEL.**

**Ramesh A.Gadekar<sup>1</sup>, Ajay D. Shinde<sup>2</sup>, Amol P. Kale<sup>3</sup>**

<sup>1</sup>Department of Pharmaceutics, Pune District Education Association's Seth Govind Raghunath Sable College of Pharmacy, Saswad, Pune, Maharashtra State – 412 301, India.

<sup>2</sup>Department of Pharmaceutics, Shivnagar Vidya Prasarak Mandal's College of Pharmacy, Malegaon Bk., Baramati, Pune, Maharashtra State – 413 115, India.

<sup>2</sup>Department of Pharmaceutics, Pune District Education Association's Seth Govind Raghunath Sable College of Pharmacy, Saswad, Pune, Maharashtra State – 412 301, India.

<sup>3</sup>Department of Pharmaceutical Chemistry, Pune District Education Association's Seth Govind Raghunath Sable College of Pharmacy, Saswad, Pune, Maharashtra State – 412 301, India.

### **Corresponding Author**

**Mr. Ramesh Abhimanyu Gadekar**

**rameshg1506@gmail.com**

**+91-9881254792**

**Department of Pharmaceutics, Pune District Education Association's Seth Govind Raghunath Sable College of Pharmacy, Saswad, Pune, Maharashtra State – 412 301, India.**

## Article History

Volume 6, Issue 7, April 2024

Received:3 June 2024

Accepted: 20 June 2024

Published: 27June 2024

doi: 10.48047/AFJBS.6.7.

2024.2617- 2663

### ABSTRACT

The Preformulation study conducted for optimizing and validating Bovine Insulin-loaded nanofiber gel formulations involved a comprehensive analysis of various parameters. FTIR spectra confirmed the compatibility of Bovine Insulin with chitosan and sodium alginate, indicating no significant interaction between the drug and polymers. DSC analysis revealed insights into the thermal behavior of Bovine Insulin powder, suggesting a transition at around 51.98°C. X-ray diffraction studies indicated a reduction in peak intensity, hinting at increased solubility and a transition from crystalline to amorphous nature in Bovine Insulin. Determination of thiol groups highlighted the presence of free thiol groups in chitosan and sodium alginate conjugates, with the addition of EDAC enhancing thiol group content. Evaluation of nanofibers demonstrated high drug entrapment efficiency and swelling index, crucial for drug loading and release behavior. Further characterization involved IR spectroscopy, DSC compatibility studies, SEM imaging, TGA analysis, and rheological studies, providing a comprehensive understanding of the formulated nanofiber gels. Moreover, optimization through PEO-loaded nanofiber gel showcased enhanced viscosity, spreadability, extrudability, and drug content uniformity, coupled with favorable drug release profiles, affirming its potential for efficient nasal drug delivery.

**KEYWORD:** Electrospun nanofiber, Central composite design, PEO loaded In situ nasal gel, stability study, In-vivo activity.

## INTRODUCTION

In the pharmaceutical industry, creating new drug delivery methods is a major issue for academics and companies. A great deal of research has been done on a number of developing technologies in order to better understand them, develop their qualities, and discover their potential. Recent years have seen a substantial growth in the number of research undertaken on nanofibers, indicating their growing interest. The adaptability of nanofiber materials in a variety of industries, such as tissue engineering, medication delivery, filtration, sensors, and more, is responsible for this exponential expansion. [1-4] Depending on the intended morphologies and uses, many methods, including template synthesis, drawing, centrifugal spinning, and electrospinning, are used to synthesize nanofibers.[5] The most practical method for creating nanofibers is electrospinning because of its ease of use, versatility, and the naturally high surface area to volume ratio in electrospun fibers. During the electrospinning procedure, a high-voltage capillary needle containing a polymer is inserted. The polymer is stretched by the electric field, forming finely nanoscale fiber mats on a granular collector. The electrospinning process is influenced by many variables, such as voltage, collector distance, flow rate, and the chemical and

physical properties of the polymer. Although these factors may be adjusted, it is still a difficult task to successfully regulate each one in order to get the appropriate nanofiber qualities. [6] In electrospinning techniques, polymers are widely used to produce a variety of nanofiber shapes, which may be obtained by adjusting polymer mixes and production conditions. For some applications, such as drug administration, where characteristics like hydrophilicity, biodegradability, and biocompatibility are critical, choosing the right polymers is key. [7] One of the most difficult tasks confronting pharmaceutical scientists today is nasal medication delivery. When a medicine is administered orally and has an unwanted side effect, nasal therapy is far more effective. When it comes to pharmacokinetics, intranasal delivery improves bioavailability by avoiding first-pass metabolism and delaying partial absorption in the gastrointestinal system. [8] The outstanding physicochemical properties of chitosan (CS) and certain of its derivatives have made them interesting for use in electrospinning. With anti-algal, anti-fungal, and anti-microbial qualities, CS is a naturally occurring polymer derived from the partial deacetylation of crustacean waste. The presence of amine and hydroxyl functional groups in CS makes it suitable for the adsorption of hazardous metals; nevertheless, the low chain flexibility, poor mechanical characteristics, and high viscosity of CS make electrospinning CS very tough and problematic. [9-11] Combining CS with polymers like polyethylene oxide (PEO) improves the mechanical characteristics of CS nanofibers.[12] In order to make CS more spinnable, it was mixed with PEO, a synthetic polymer that is biocompatible, semi-crystalline, and bioadhesive due to its hydrogen bonding capabilities.[13-14]. PEO is one of the most preferred polymers for producing nanofibrous membranes for use in biomedical and healthcare applications, such as drug delivery, wound healing, and scaffolds.

## **MATERIALS AND METHODS:**

### **MATERIALS:**

Bovine Insulin, chitosan, EDAC, cysteine, sodium alginate, sodium hydroxide, sodium acetate, 5,5'-dithiobis (2-nitrobenzoic acid), sodium carboxymethyl cellulose, methanol, acetonitrile, hydrochloric acid (HCl) 32%, o-phosphoric acid 85%, phenol-extra pure, m-cresol – pure, o-nitrophenol 99%, and potassium Dihydrogen phosphate were purchased from Cosmo Chem. Pvt. Ltd. Tris (2-carboxyethyl) phosphine hydrochloride was purchased from Merck Pvt. Ltd. Polyethylene oxide (PEO) was purchased from Akshar Chem. Pvt. Ltd.

## **METHODS:**

### **Formulation and Development**

#### **Preparation of Polymer Conjugates (Thiomers)**

##### **Synthesis of chitosan conjugate [15]**

Chitosan (500 mg) was dissolved in 4 mL of 1M HCl and then diluted with demineralized water to obtain a 1% (w/v) polymer solution. Ethyl (dimethylaminopropyl) carbodiimide (EDAC) was added to achieve a final concentration of 200 mM. After 20 minutes, varying amounts of N-acetyl cysteine (4 gm) were slowly added under stirring. For reactions involving aromatic ligands, tris (2-carboxyethyl) phosphine hydrochloride (TCEP) was added at a final concentration of 10 mM as a reducing agent. The pH was adjusted to 5 with 1M NaOH, and the reaction proceeded for 5 hours at room temperature with vigorous stirring. After dialysis, the pH was readjusted to 4, and the solutions were freeze-dried at 77°C and 0.01 mbar, then stored at 4°C until further use.

##### **Synthesis of sodium alginate conjugate-[16]**

Sodium alginate (500 mg) was dissolved in 4 mL of 1M HCl and diluted with demineralized water to create a 1% (w/v) polymer solution. Ethyl (dimethylaminopropyl) carbodiimide (EDAC) was then added to achieve a final concentration of 200 mM. After 20 minutes, varying amounts of N-acetyl cysteine (4 gm) were slowly added under stirring. For reactions involving aromatic ligands, tris (2-carboxyethyl) phosphine hydrochloride (TCEP) was added at a final concentration of 10 mM as a reducing agent. The pH was adjusted to 5 with 1M NaOH, and the reaction proceeded for 5 hours at room temperature with vigorous stirring. After dialysis, the pH was readjusted to 4, and the solutions were freeze-dried at 77°C and 0.01 mbar, then stored at 4°C until further use.

##### **Determination of Thiol Group Contents with Ellman's Reagent method.**

Content of free thiol groups immobilized on chitosan can be determined by spectrophotometry using Ellman reagent [5,5'-dithiobis (2-nitrobenzoic acid)] (DTNB). Before determining the content of thiol groups in the sample must be made the solution of cysteine standard curve:

## **For Chitosan conjugate**

### **Preparation of standard calibration curve of N-Acetyl Cysteine [17]**

A DTNB stock solution containing 50 mM sodium acetate and 2 mM DTNB was prepared using molecular biology grade water. A 1 M Tris solution with pH adjusted to 8.0 was then made. Cysteine standard solutions starting at a concentration of 10  $\mu\text{M}$  were prepared. For each measurement, 10  $\mu\text{L}$  of cysteine standard solution was combined with 50  $\mu\text{L}$  of DTNB solution, 100  $\mu\text{L}$  of Tris solution, and aqua bidestilata to reach a final volume of 1000  $\mu\text{L}$ . After mixing and a 5-minute incubation at room temperature, absorbance was measured at 412 nm. Dilutions were made from the final volume to prepare 100  $\mu\text{L}$  of solution, and solutions ranging from 10-60  $\mu\text{L}$  were prepared. Absorbance was measured for each to generate a regression equation.

### **Preparation of sample solution**

Sample solution prepared by dissolving 50 mg of chitosan conjugate in 25 mL of Nuclease-Free Water. Amount of 10  $\mu\text{L}$  of sample solution is inserted into a measuring flask, then added 50  $\mu\text{L}$  DTNB solution, 100  $\mu\text{L}$  solution of Tris, and of Nuclease-Free Water until the final volume of 1000  $\mu\text{L}$ . Solution was mixed well and incubated at room temperature for 5 minutes, then absorbance was measured at a wavelength of 412 nm. Absorbance obtained subsequently incorporated into the regression equation of standard solution of cysteine thus obtained concentration of the sample being examined.

## **For sodium alginate**

### **Solution of cysteine standard curve: [18]**

DTNB stock solution containing 50 mM sodium acetate and 2 mM DTNB prepared using molecular biology degree water (aqua bidestilata). Tris solution was then made with a final concentration of 1 M and its pH adjusted to 8.0. A series of cysteine standard solution was made starting at a concentration of 10  $\mu\text{M}$ . Amount of 10  $\mu\text{L}$  standard solution of cysteine inserted into the measuring flask, then added 50  $\mu\text{L}$  DTNB solution, 100  $\mu\text{L}$  solution of Tris, and aqua bidestilata until the final volume of 1000  $\mu\text{L}$ . Solution was mixed well and incubated at room temperature for 5 minutes, then absorbance was measured at a wavelength of 412 nm. Absorbance obtained and graphed against concentration to obtain the regression equation.

### **Preparation of calibration curve**

From the final volume of 1000  $\mu\text{L}$ , dilutions were made to prepare 100  $\mu\text{L}$  of the solution and simultaneously 10-60  $\mu\text{L}$  solutions were made. The absorbances were obtained to generate regression equation.

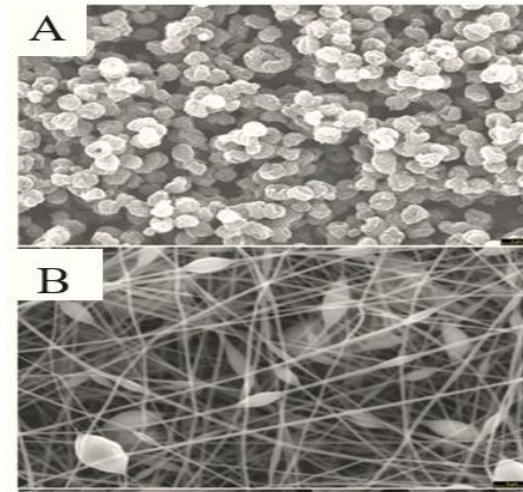
### **Preparation of sample solution**

Sample solution prepared by dissolving 50 mg of sodium alginate conjugate in 25 mL of Nuclease-Free Water. Amount of 10  $\mu\text{L}$  of sample solution is inserted into a measuring flask, then added 50  $\mu\text{L}$  DTNB solution, 100  $\mu\text{L}$  solution of Tris, and of Nuclease-Free Water until the final volume of 1000  $\mu\text{L}$ . Solution was mixed well and incubated at room temperature for 5 minutes, then absorbance was measured at a wavelength of 412 nm. Absorbance obtained subsequently incorporated into the regression equation of standard solution of cysteine thus obtained concentration of the sample being examined.

### **Preparation of Nanofiber [19]**

PVA and PEO were dissolved in chitosan and sodium alginate conjugate thiomers solution at the concentrations of 8mg/ml. The solution was stirred for 72 hours at room temperature, allowing all solid components to completely solubilize. Bovine Insulin powder was then added at a final concentration of 2.8 mg/ml. At the given concentration, Bovine Insulin dissolved rapidly to produce a translucent solution of uniform color and viscosity.

Many trials on following conditions were studied to Optimize the nanofiber formation method. 10, 15, 20Kv DC offset, 13,15 and 17 cm air gap and 1,3 and 5ml/h flow rate studied, of which at 15 kV DC offset, 17 cm air gap, 18 ga. blunted needle, and 3 ml/h flow rate the desired size nanofibers were formed.



The above figures shows, A) the nanofibers formed at 10 Kv DC offset, 13 cm air gap and 1ml/h flow rate whereas B) the nanofibers formed at 20 Kv DC offset, 15 cm air gap and 5ml/h flow rate, which confirms that there is no proper formation of nanofibers at set conditions. Whereas the nanofibers formed at 15 kV DC offset, 17 cm air gap, 18 ga. blunted needle, and 3 ml/h flow rate showed good size nanofibers formation, so the above condition was considered as Optimized condition. The solution was electrospun into solid fiber mats under the following conditions: 15 kV DC offset, 17 cm air gap, 18 ga. blunted needle, and 3 ml/h flow rate. A typical spinning run used 5 ml of solution and a round collecting mandrel (6.5 mm diameter). Scaffolds were dried under vacuum 3 hours to remove residual solvent before any further testing.

**Table 1: Optimized Formulation Table of Nanofibre Synthesis**

<b>Batch Name</b>	<b>Chitosan Thiomer (ml)</b>	<b>Sodium alginate Thiomer (ml)</b>	<b>PEO (mg/ml)</b>	<b>PVA (mg/ml)</b>	<b>Bovine Insulin Powder (mg)</b>
<b>NF1</b>	-	<b>20</b>	<b>8</b>	-	<b>2.8</b>
<b>NF2</b>	-	<b>20</b>	-	<b>8</b>	<b>2.8</b>
<b>NF3</b>	<b>20</b>	-	<b>8</b>	-	<b>2.8</b>
<b>NF4</b>	<b>20</b>	-	-	<b>8</b>	<b>2.8</b>

### **Preparation of In-Situ Gel Containing Electrospun Nanofibres**

To prepare the gel, started by dissolving 0.4 g of sodium carboxy methyl cellulose (CMC) in a small amount of a buffer solution with a pH of 7.4. Ensured thorough dissolution by continuous stirring. Separately, dispersed 4.0 mg of drug-loaded nanofibers into the CMC solution, achieving a uniform mixture by employing a homogenizer to ensure the nanofibers are well-distributed. Adjusted the gel's consistency by adding small amounts of either CMC / buffer solution until the desired texture is reached, stirring after each addition. Verified the pH of the final gel, making adjustments with additional buffer solution.

### **Formulation and optimization using central composite design (CCD) of PEO [20]**

In the current study, a Response Surface Methodology (RSM) known as Central Composite Design (CCD) was employed using Design Expert® software (Version 13.0). The CCD was applied with three independent variables: the amount of PEO+Sodium alginate (A), PEO+Chitosan (B), and Sodium carboxymethyl cellulose (C). The dependent variables under investigation in this study are pH and Spreadability. This CCD design incorporated factorial points, a center point, and axial points, resulting in a total of 15 runs. The details of the independent variables, their coded levels, and the scheme matrix of the CCD can be found in the provided table.

**Table 2: DOE Suggested batches of PEO**

<b>Formulation Code</b>	<b>PEO + Sodium Alginate Nanofiber (mg)</b>	<b>PEO + Chitosan Nanofiber (mg)</b>	<b>Sodium Carboxy Methyl Cellulose (mg)</b>	<b>Buffer pH 7.4 Q.S. to (gm)</b>
<b>NGB 1</b>	4	2	0.2	10
<b>NGB 2</b>	3	3	0.3	10
<b>NGB 3</b>	4	4	0.4	10
<b>NGB 4</b>	3	3	0.468179	10
<b>NGB 5</b>	2	4	0.2	10

<b>NGB 6</b>	4	4	0.2	10
<b>NGB 7</b>	2	2	0.4	10
<b>NGB 8</b>	3	1.31821	0.3	10
<b>NGB 9</b>	4.68179	3	0.3	10
<b>NGB 10</b>	3	3	0.131821	10
<b>NGB 11</b>	2	2	0.2	10
<b>NGB 12</b>	4	2	0.4	10
<b>NGB 13</b>	2	4	0.4	10
<b>NGB 14</b>	1.31821	3	0.3	10
<b>NGB 15</b>	3	4.68179	0.3	10

### **Preformulation Study**

#### **FOURIER-TRANSFORM INFRARED SPECTROSCOPY (FTIR) [21]**

Using Fourier transform infrared spectroscopy, the IR spectrum of Bovine Insulin was recorded and compared to drug reference spectra. Sample was placed on the sample platform and squeezed between the knob and sample platform. The spectrum of infrared light was measured between 500 and 3500 cm<sup>-1</sup>.

#### **Differential Scanning Calorimetry (DSC) [22]**

Differential scanning calorimetric (DSC) measurements were carried out on a modulated DSC (Mettler Toledo, SW STARe, USA). Samples were weighed (2-8mg), the aluminum pans were used and hermetically covered with lead. The heating range was 50-250 °C for sample with constant increasing rate of temperature at 10°C /min under nitrogen atmosphere (50-

60ml/min). The resultant thermograms of formulation was obtained. The Bovine Insulin powder, Chitosan loaded-NF3 and Sodium alginate loaded –NF1 formulation, these samples were studied for DSC.

### **X- ray diffraction study (XRD) 23]**

The structural composition can be studied using X-ray diffraction method. bovine Bovine Insulin powder samples were ground to fine powder and spectra were recorded on Bruker XRD Instrument using the source Copper K alpha.X-ray Powder diffraction measurements is used to confirm the crystalline nature and glass formation of the sample. A XPERT-PRO diffractometer system with a rotating anode Cu Ka was used and scans are taken between 5 °C and 100 °C.

### **Evaluation and Characterization of nanofiber**

#### **Evaluation of nanofiber**

#### **Drug entrapment efficiency [24]**

The ultra-centrifugation technique was used to assess the drug entrapment effectiveness of nanofiber formulations. Using ultracentrifugation at 10,000 rpm for 30 minutes. The pellets were re-dissolved in distilled water, and the supernatant was scanned with a UV-visible spectrophotometer in this parameter.

The drug encapsulation efficiency was determined by using the relation in this equation.

$$\% \text{ Drug entrapment efficiency} = \text{experimental drug content} \times 100 / \text{Theoretical drug content}$$

#### **Swelling index [25]**

Swelling capacity of the nanofibres samples was investigated by direct immersion of formulations in PBS (pH 7.4) to simulate medium conditions. The swelling degree (S) was calculated according to

$$S (\%) = \{(wt - wd)/wd\} \times 100 \dots\dots\dots (1)$$

Where wt. is the weight of the swollen sample at time t and Wd is the initial weight of the dry sample.

#### **Characterization of nanofiber**

**Fourier-transform infrared spectroscopy (FTIR) [24]**

FTIR spectroscopy was used in the range 400-4000  $\text{cm}^{-1}$  to determine the type of functional groups on the prepared nanofibre. Dried nanofibers were mixed with KBr powder and pelletized. The IR characterizations were performed using a Perkin-Elmer Spectrum GX FTIR spectrometer.

**Differential Scanning Calorimetry (DSC) [26]**

Differential scanning calorimetric (DSC) measurements were carried out on a modulated DSC (Mettler Toledo, SW STARE, USA). Samples were weighed (2-8mg), the aluminum pans were used and hermetically covered with lead. The heating rate was 50-250  $^{\circ}\text{C}$  for sample with constant increasing rate of temperature at 10 $^{\circ}\text{C}$  /min under nitrogen atmosphere (50-60ml/min). The resultant thermograms of formulation was obtained. The Bovine Insulin powder, Chitosan loaded-NF3 and Sodium alginate loaded –NF1 formulation, these samples were studied for DSC. [307]

**Scanning electron microscope (SEM) [27]**

The Scanning electron microscope (SEM, Zeiss, Japan) was used to observe the morphology and diameter of the NF1 nanofibers, NF2 nanofibers, NF3 nanofibers and NF4 nanofibers electrospun nanofibers. In this study the samples image were captured at the accelerating voltage of 5 kV under the magnification of 17.42 X. The synthesized nanofibers were cut into small pieces and coated on a gold sputter (sputter coater: Emitech SC7620) in order to prevent charging and improve the resolution of the image. The average fiber diameter was measured with the SEM images.

**TGA [28]**

The thermal stability and the fraction of the volatile components of the synthesized nanofiber A) NF1 B) NF2 C) NF3 D) NF4 were analyzed with the help of Thermo Gravimetric Analyzer (TGA) (PERKIN – ELMER TG – DTA). The samples were heated at constant heating rate at 10 $^{\circ}\text{C}$  / min from room temperature to 800 $^{\circ}\text{C}$  under nitrogen ( $\text{N}_2$ ) atmosphere at a purging rate of 100 ml / min. During the process the weight of the samples were measured, it was not degraded, no change in weight during the desired temperature of the polymer and also no slope was

observed in the TGA graph with negligible changes of the samples. If the samples were degraded the weight will decrease and if the weight will increase because the samples were reacted with oxygen.

### **Characterization of In-Situ Gel Containing Electrospun Nanofibres**

#### **Determination of pH [29]**

The pH of the Nanogels was determined by using digital pH meter which was previously calibrated by standard solution prepared by standard capsules of pH 4, 7 and 9.2 respectively. pH measurement of the gels was carried out by dipping the pH-electrode of a digital pH meter completely into the gel formulation for 10 min prior to taking the readings in order to allow the pH values to stabilize. The measurement was carried out in triplicate, and the average of the three readings was recorded. The electrode was washed thoroughly between each reading.

#### **Determination of Viscosity [30]**

The viscosity of the Nanogels was determined by using Brookfield viscometer with spindle no. 64, rotated at 5 rpm for 5 min at 25 °C temperature.

#### **Determination of Spreadability [31]**

The spreadability of Nanogels was determined using the "maximum slip and minimum drag" principle. Excess gel formulation was placed between two glass slides, and a 1000 g weight was applied for 1 minute to expel air and ensure uniform distribution. After removing the weight, excess gel was scraped off the edges. The lower slide was fixed, while the upper slide was attached to a string connected to a pan with an 80 g weight. Pulling the upper slide measured the time it took to separate the two slides, indicating spreadability.

The experiments were done in triplicate.

The following formula is used to calculate the spreadability.

$$S = m \times l t \dots\dots\dots (2)$$

Where, S is the Spreadability, m is that the weight tied to the upper slide (g), l is the length of a glass slide (cm), t is the time taken to separate the slide completely from each other (s).

#### **Extrudability [32]**

The extrudability of Nanogels was determined by the amount of gel extruded from the tube on the application of pressure. The formulation was filled in a clean lacquered collapsible aluminum tube of capacity 5 g with 5 mm orifice, and the tube is pressed firmly at the crimped end, and the clamp was applied to prevent any rollback. The amount of extruded gel was collected carefully and weighed accurately. Extrudability was then determined by measuring the amount of gel extruded (in percentage) through the orifice when a pressure was applied to the tube. The experiment was performed in triplicate.

### **Drug Content Uniformity [33]**

To ensure uniform distribution of the drug entrapped in nanofibers within the gel, samples were collected from different locations (top, middle, and bottom) of the tube. Each sample weighing 0.250 g was accurately transferred to a 250 ml volumetric flask and diluted with 100 ml methanol to break the nanofiber structure. The flask was vigorously shaken for 30 minutes on a mechanical shaker to disperse the gel, followed by 10-15 minutes of sonication for complete drug extraction. The solutions were then filtered and analyzed by UV-Vis spectrophotometer (Jasco V-630) to determine drug content using a standard calibration curve.

### **In-Vitro drug diffusion study [34]**

Cellophane membrane diffusion technique was used to study in-vitro diffusion of drug from the prepared nanogel formulations. The receptor medium used was freshly prepared phosphate buffer pH 7.5. Cellophane membrane soaked overnight in the receptor medium was on the Franz's Diffusion cell assembly 0.5 g of formulation was placed in the donor compartment and the assembly was kept on the multistation diffusion study apparatus (make Orchid Scientific) at  $37^{\circ}\text{C} \pm 2^{\circ}\text{C}$  and stirred at 700 RPM. Aliquots of 0.5 ml were withdrawn at pre-determined time intervals (0.5, 1, 2, 4, 8, and 12 hrs.) and immediately replaced by same volume of the fresh medium. The aliquots were suitably diluted with the dissolution medium and analyzed by UV-Vis Spectrophotometer at 276nm ( $\lambda_{\text{max}}$ ). The data obtained from the in-vitro diffusion studies were fitted to various kinetic equations to find out the mechanism of drug release from the Nanogels.

### **In-vivo activity [35-36]**

#### **Streptozotocin (STZ) Induced Antidiabetic Activity:**

**Animal Selection:**

Wistar albino rats weighing 220 to 250g were chosen for the study.

**Preparation of Trisodium Citrate:**

Weighed accurately 8.4gm of Trisodium Citrate Dihydrate (TCD) using a weighing balance. Then measured TCD was added to a clean container and in this container 200ml of distilled water was poured and stirred the mixture until the TCD is completely dissolved. Afterwards to adjust the PH 4.5, started by adding a small amount of citric acid (around 0.5gms) to the solution. Then stirred and checked the pH using PH meter. Repeated this process until the pH reaches to 4.5. After adjusting the pH of 4.5 diluted the solution with additional distilled water to make up the final volume 250ml with thorough mixing.

**Diabetes Induction:**

Diabetes was induced in overnight fasted rats by injecting 0.5ml streptozotocin (50mg/kg) intraperitoneally (i.p). Streptozotocin is a compound known for inducing diabetes in experimental animals.

**Selection Criteria for Diabetic Rats:**

Seven days after streptozotocin injection, rats with blood glucose levels more than 200 mg/dL were selected.

**Group Division:**

After an overnight fast, rats were divided into five groups (n = 6).

**Group 1:** Control rats orally administered with distilled water (10ml /kg) (p.o.).

**Group 2:** Streptozotocin-induced diabetic rats administered orally with distilled water.  
(50 mg/kg) (p.o.)

**Group 3:** Streptozotocin-induced diabetic rats administered orally with Metformin dissolved in distilled water (20 mg/kg).

**Group 4:** Streptozotocin-induced diabetic rats received nanofiber loaded intranasal in gel (NGA 5) form (1.5 IU/kg) using a micro syringe attached to a blunt needle with a 0.5-inch polyethylene tube at the end.

**Group 5:** Streptozotocin-induced diabetic rats received nanofiber loaded intranasal in gel (NGB3) form (1.5 IU/kg) using a micro syringe attached to a blunt needle with a 0.5-inch polyethylene tube at the end.

#### **Blood Collection and Glucose Measurement:**

At specified time intervals (On day 0, 7, 14, 28 after treatment) blood was collected from orbital sinuses. Blood glucose levels were determined using a digital glucometer.

#### **Stability Study [37]**

Accelerated stability studies of optimized nanogel was carried out according to ICH Q1A (R2) guidelines. The stability study was performed at  $25 \pm 2^\circ\text{C}$  and  $60 \pm 5\%$  RH in an environmental stability chamber over a period of three months to assess the stability of nanogel. The nanogel was transferred to amber-colored glass vials, which were plugged and kept in the stability chamber. The drug content, viscosity and Entrapment efficiency measured after three months.

## **RESULTS AND DISCUSSION**

### **PREFORMULATION STUDY**

#### **Optimization and Validation of Bovine Insulin by HPLC**

#### **FTIR spectra of Bovine Insulin**

The FTIR studies showed that the significant peaks of Bovine Insulin are O-H stretching at  $1390.32\text{ cm}^{-1}$ , C=O vibration at  $1642.49\text{ cm}^{-1}$  and C-H [CH<sub>2</sub>] bending at  $1445.45\text{ cm}^{-1}$  and C-O-C at  $1079.93\text{ cm}^{-1}$ , NH cm<sup>-1</sup> at  $3268.41\text{ cm}^{-1}$ . Based on that FTIR spectrum of Bovine Insulin functional groups peak was coincided with standard Insulin pure drug. Based on this result the drug was confirmed as in its pure form without by-products.

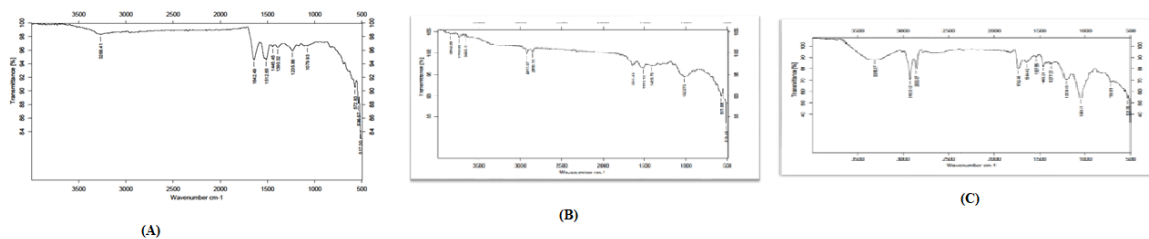
#### **FTIR Spectrum of Bovine Insulin and chitosan loaded nanofibres solution**

The FTIR studies showed that the significant peaks of Bovine Insulin are C=O vibration at  $1641.84\text{ cm}^{-1}$  and C-H [CH<sub>2</sub>] bending at  $1415.78\text{ cm}^{-1}$  and C-O –C at  $1022.72\text{ cm}^{-1}$ , NH cm<sup>-1</sup> at  $3265.11\text{ cm}^{-1}$ . Based on that FTIR spectrum of Bovine Insulin functional groups peak was

coincided with standard Insulin pure drug. The IR spectra did not show any difference in wavelength from those obtained for their physical mixture with polymers as compared to drug. These obtained results indicate that there was no interaction between Bovine Insulin and chitosan polymers and the other excipients. Hence they are compatible with each other. Thus, Bovine Insulin can be used in combination for the preparation gel.

### **FTIR Spectrum of Bovine Insulin and sodium alginate loaded nanofiber solution**

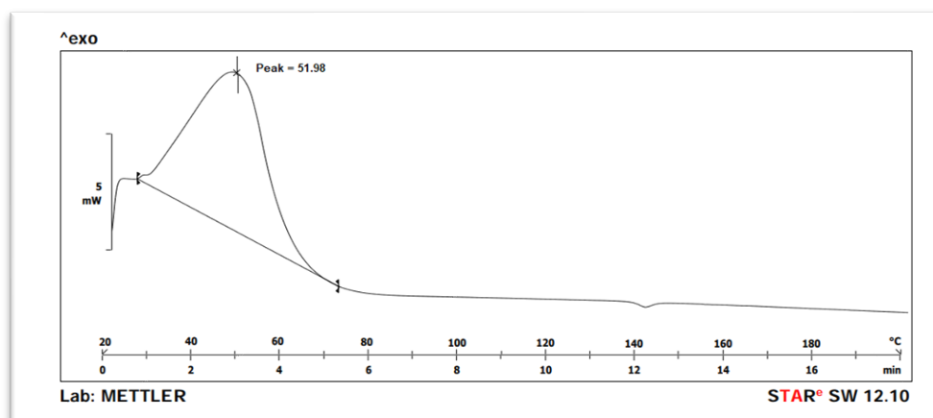
The FTIR studies showed that the significant peaks of Bovine Insulin are C=O vibration at 1644.42 cm<sup>-1</sup> and C-H [CH<sub>2</sub>] bending at 1463.21 cm<sup>-1</sup> and C-O-C at 1049.51 cm<sup>-1</sup>, NH cm<sup>-1</sup> at 3309.47 cm<sup>-1</sup>. Based on that FTIR spectrum of Bovine Insulin functional groups peak was coincided with standard Insulin pure drug. The IR spectra did not show any difference in wavelength from those obtained for their physical mixture with polymers as compared to drug. These obtained results indicate that there was no interaction between Bovine Insulin and sodium alginate polymers and the other excipients. Hence they are compatible with each other. Thus, Bovine Insulin can be used in combination for the preparation gel.



**Figure 1: (A) FTIR Spectrum of Bovine Insulin (B) FTIR Spectrum of Bovine Insulin and chitosan loaded nanofibres solution, (C) FTIR Spectrum of Bovine Insulin and sodium alginate loaded nanofiber solution**

### **DSC Compatibility study (Drug-Excipients)**

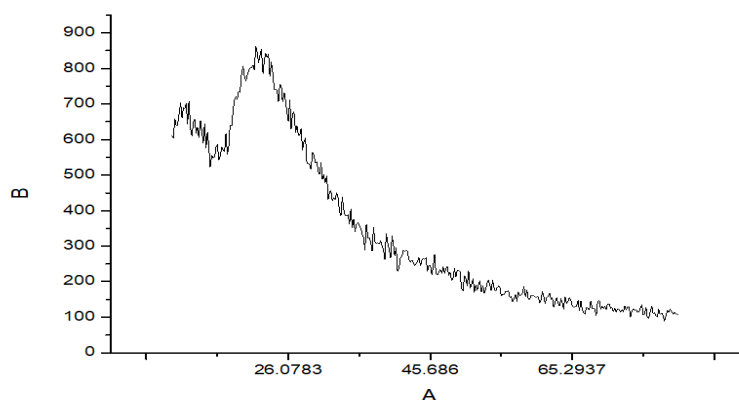
The observation of a peak at 51.98°C in the DSC (Differential Scanning Calorimetry) thermograms of Bovine Insulin provides valuable insights into its thermal behavior and stability. The peak observed at 51.98°C indicates a thermal event or transition occurring within the sample at this temperature.



**Figure 2: DSC spectrum of Bovine Insulin powder**

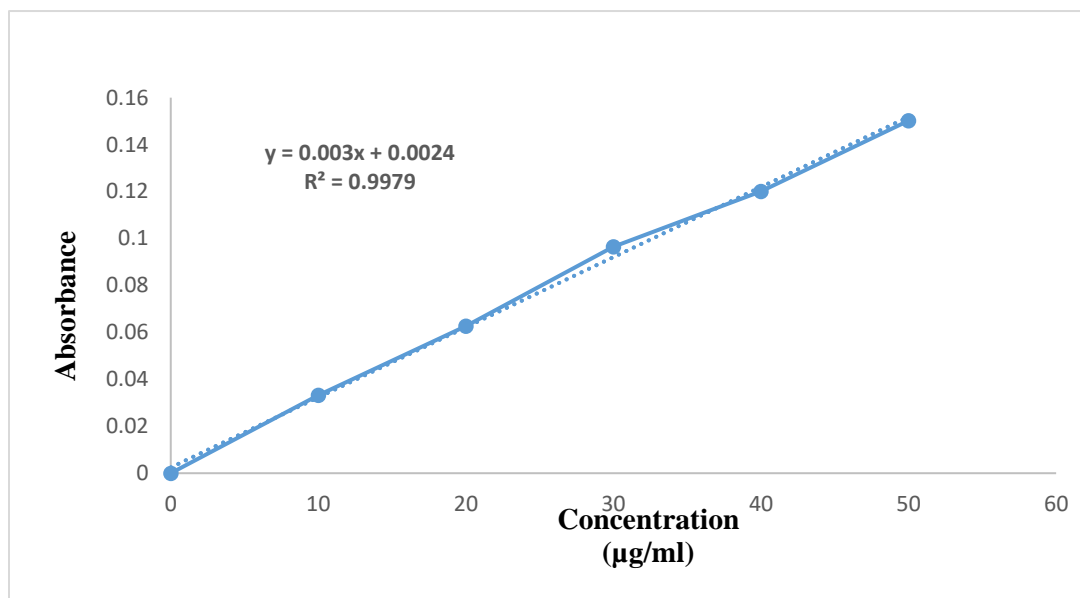
### **X- ray diffraction study of Bovine Insulin:**

The characteristic peaks of Bovine Insulin powder were centered at  $2\theta = 26.0783$  corresponding to the crystallographic planes respectively. The XRD analysis of Bovine Insulin powder indicates a reduction in peak intensity, suggesting an increase in solubility and a conversion from crystalline to amorphous nature.



**Figure 3: X-ray diffraction patterns of Bovine Insulin****DETERMINATION OF THIOL GROUP****Preparation of Standard Calibration Curve of N-Acetyl Cysteine:****Table 3: Calibration Curve of N-Acetyl Cysteine**

Concentration ( $\mu\text{g/ml}$ )	Absorbance
0	0.0000
10	0.03320
20	0.06269
30	0.09654
40	0.12010
50	0.15020

**Figure 4: Calibration curve of cysteine****For Chitosan conjugate**

Contents of thiol groups in the chitosan conjugate is calculated by inserting the sample absorbance of chitosan conjugate were read in the Uv-vis spectrophotometer into the regression equation curve standard solution of cysteine, i.e.  $y = 0.003x + 0.0024$ ;  $R^2 = 0.9979$ . Absorbance data and concentration of free thiol groups in the sodium alginate conjugate can be seen in Table.

**Table 4: Absorbance and content of free thiol groups in the 50 mg of chitosan conjugate**

Sample name	Absorbance of sample	Concentration of sample (Unit)
Chitosan conjugate (without EDAC)	0.017	4.867
Chitosan conjugate (with EDAC) 200mM	0.5986	198.733

The results showed that there are free thiol groups present, which are formed. Chitosan and sodium alginate conjugates by the addition of EDAC 200mM has the highest content of thiol groups of conjugates. EDAC acts as a catalyst in the formulation of chitosan conjugates. The results showed that chitosan and sodium alginate conjugates have a thiol group, it became evident that the amide bond formed between chitosan and sodium alginate.

#### **For Sodium alginate conjugate**

Contents of thiol groups in the sodium alginate conjugate is calculated by inserting the sample absorbance of sodium alginate conjugate were read in the uv-vis spectrophotometer into the regression equation curve standard solution of cysteine, i.e.  $y = 0.003x + 0.0024$ ;  $R^2 = 0.9979$ . Absorbance data and concentration of free thiol groups in the sodium alginate conjugate can be seen in Table.

**Table 5: Absorbance and content of free thiol groups in the 50 mg of sodium alginate conjugate**

Sample name	Absorbance of sample	Concentration of sample (Unit)
Sodium alginate conjugate (without EDAC)	0.008	1.887

Sodium alginate conjugate (with EDAC) 200mM	0.5986	198.733
--	--------	---------

The results showed that there are free thiol groups present, which are formed. Chitosan and sodium alginate conjugates by the addition of EDAC 200mM has the highest content of thiol groups of conjugates. EDAC acts as a catalyst in the formulation of chitosan conjugates. The results showed that chitosan and sodium alginate conjugates have a thiol group, it became evident that the amide bond formed between chitosan and sodium alginate.

### Evaluation and Characterization of Nanofibers:

#### Evaluation of Nanofibers:

#### Drug entrapment efficiency

The entrapped efficiency of different formulations (NF1, NF2, NF3, NF4):

**Table 6: Determination of Entrapment efficiency (%) of Nanofiber NF1-NF4**

Sr. No.	Batch Code	Entrapment Efficiency (%)
1.	NF1	75.22±0.770
2.	NF2	77.20±0.560
3.	NF3	78.45±0.140
4.	NF4	85.12±0.890

#### Swelling Index Determination:

**Table 7: Swelling Index**

Sr. No.	Batch Code	Swelling (%)
---------	------------	--------------

1.	NF1	64.44±0.01
2.	NF2	78.59±0.02
3.	NF3	76.06±0.12
4.	NF4	88.62±0.05

The swelling index of the electrospun nanofiber materials was determined using a gravimetric method. The swelling index of the nanofiber plays an important role in the loading and release behavior of a drug. Above figure shows the degree of swelling of drug loaded nanofiber gel at different time intervals. The degree of swelling of Nano fibrous gel (NF1-NF4) in PBS pH 7.4 was 64.44, 78.59, 76.06 and 88.62 for the time intervals of 1, 2, 4, 6, 8, 10, and 12 h, respectively.

### Characterization of Nanofibers:

#### IR spectrum

#### IR spectrum of prepared nanofibers batch NF1

The FTIR studies showed that the significant peaks of Bovine Insulin are C=O vibration at 1735.84 cm<sup>-1</sup> and C-H [CH<sub>2</sub>] bending at 1464.24 cm<sup>-1</sup> and C-O-C at 1010.35 cm<sup>-1</sup>, O-H Stretch cm<sup>-1</sup> at 3648.07 cm<sup>-1</sup>. Based on that FTIR spectrum of Bovine Insulin functional groups peak was coincided with standard Insulin pure drug. The IR spectra did not show any difference in wavelength from those obtained for their nanofiber formulation as compared to drug.

#### IR spectrum of prepared nanofiber batch NF2

The FTIR studies showed that the significant peaks of Bovine Insulin are C=O vibration at 1731.49 cm<sup>-1</sup> and C-H [CH<sub>2</sub>] bending at 1468.78 cm<sup>-1</sup> and C-O-C at 1056.73 cm<sup>-1</sup>, O-H Stretch cm<sup>-1</sup> at 3666.14 cm<sup>-1</sup>. Based on that FTIR spectrum of Bovine Insulin functional groups peak was coincided with standard Insulin pure drug. The IR spectra did not show any difference in wavelength from those obtained for their nanofiber formulation as compared to drug.

#### IR spectrum of prepared nanofibers batch NF3

The FTIR studies showed that the significant peaks of Bovine Insulin are C=O vibration at 1789.57cm<sup>-1</sup> and C-H [CH<sub>2</sub>] bending at 1515.02 cm<sup>-1</sup> and C-O-C at 1053.61cm<sup>-1</sup>, O-H Stretch cm<sup>-1</sup> at 3608.89 cm<sup>-1</sup>. Based on that FTIR spectrum of Bovine Insulin functional groups peak was coincided with standard Insulin pure drug. The IR spectra did not show any difference in wavelength from those obtained for their nanofiber formulation as compared to drug.

#### **IR spectrum of prepared nanofiber batch NF4**

The FTIR studies showed that the significant peaks of Bovine Insulin are C=O vibration at 1682.50cm<sup>-1</sup> and C-H [CH<sub>2</sub>] bending at 1560.81 cm<sup>-1</sup> and C-O-C at 1031.78cm<sup>-1</sup>, O-H Stretch cm<sup>-1</sup> at 3739.89 cm<sup>-1</sup>. Based on that FTIR spectrum of Bovine Insulin functional groups peak was coincided with standard Insulin pure drug. The IR spectra did not show any difference in wavelength from those obtained for their nanofiber formulation as compared to drug.

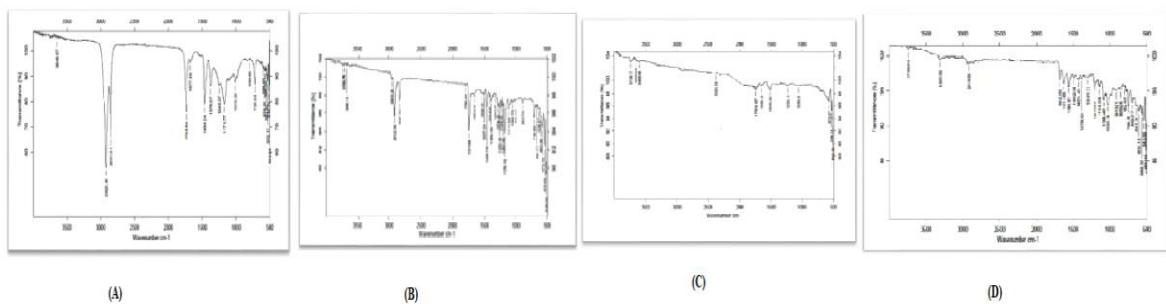


**Figure 5:**

- (A) IR spectrum of prepared nanofibers batch NF1,**
- (B) IR spectrum of prepared nanofibers batch NF2,**
- (C) IR spectrum of prepared nanofibers batch NF3,**
- (D) IR spectrum of prepared nanofibers batch NF4**

#### **DSC compatibility study**

The DSC thermograms of sodium alginate (NF1) exhibits one endothermic band at 58.41°C. The first endothermic band corresponds to the evaporation of hydration water molecules while the exothermic one indicates the oxidative degradation of alginate polymers

The observation of a peak at 63.24°C in the DSC (Differential Scanning Calorimetry) spectrum of the formulation blend (Chitosan loaded-NF3) indicates a thermal event or transition occurring within the sample at this temperature. The peak observed at 63.24°C could potentially

correspond to various phenomena depending on the specific composition and characteristics of the formulation blend:

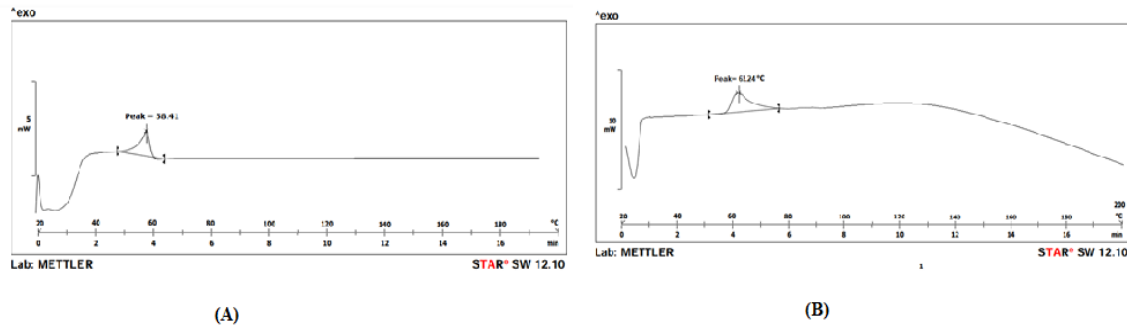
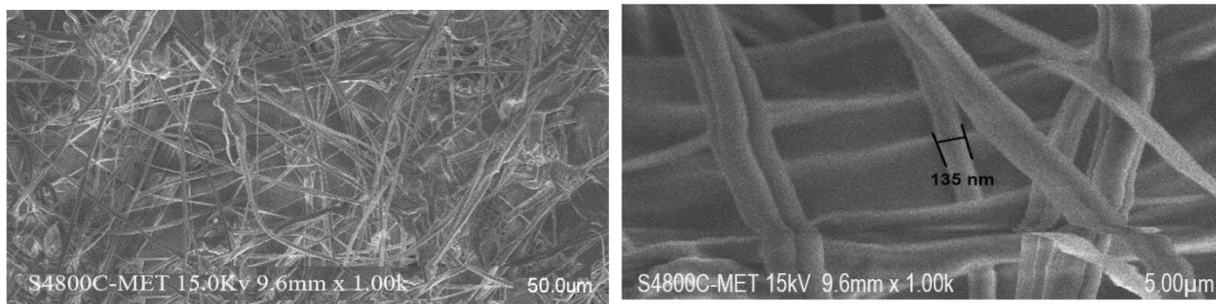


**Figure 6 : (A) DSC spectrum of formulation blend (Sodium alginate loaded –NF1) ,  
(B) DSC spectrum of formulation blend (Chitosan loaded-NF3)**

### Scanning electron microscope (SEM)

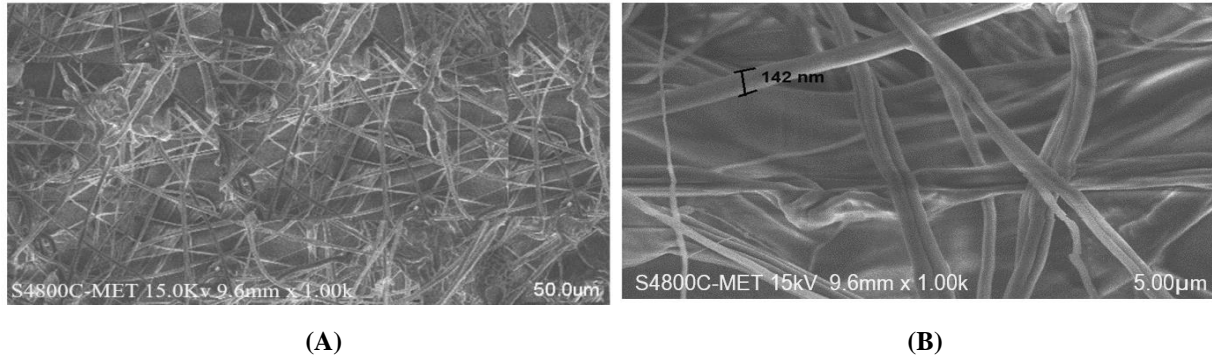
Particle shape and its arrangement inside the formulation can be unfolded by scanning electron microscopy (SEM). Scanning electron microscopy was used to examine the surface morphology of silver nanofibers. The SEM graphs are represented below. The morphology for plain and prepared nanofiber patches was analysed by using a Hitachi S-4700 SEM (scanning electron microscope Hitachi Company, Japan). Before being considered, samples were placed on metal ends using double-sided adhesive tape and vacuum-coated with a gold sputter layer. A mixed population of sub-micron ( $\sim 200$  nm) and larger ( $2\text{--}4\mu\text{m}$ ) fibers were observed for all the formulated nanofibers.



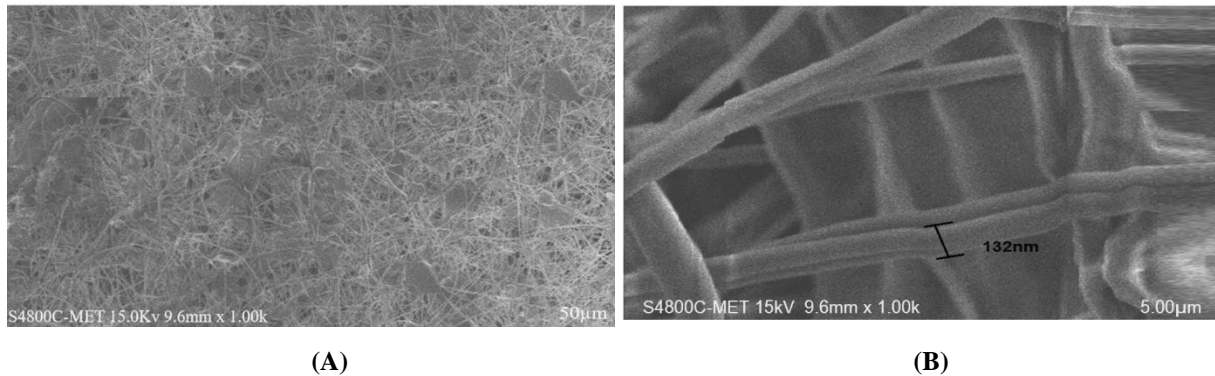
(A)

(B)

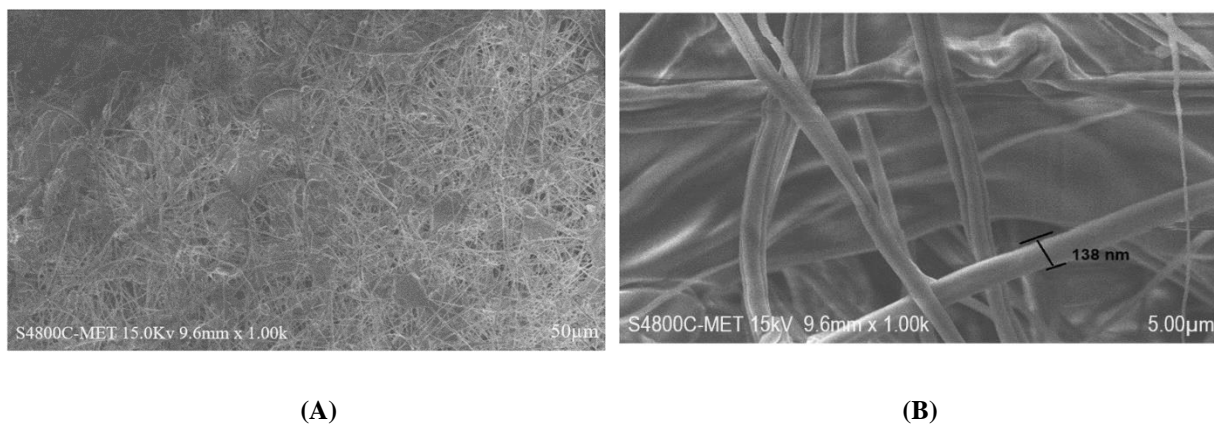
**Figure 7: Scanning electron microscopy (SEM) images of NF1 nanofibers containing sodium alginate (NF1) A) SEM image of spunbond fibers B) SEM image of electrospun fibers)**



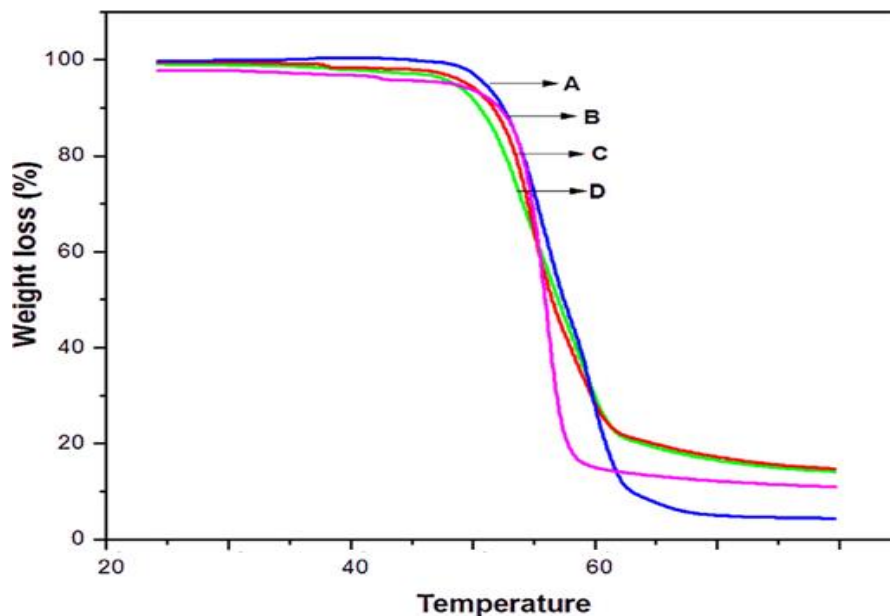
**Figure 8: Scanning electron microscopy of NF2 A) SEM image of spunbond fibers B) SEM image of electrospun fibers**



**Figure 9: Scanning electron microscopy of NF3 A) SEM image of spunbond fiber B) SEM image of electrospun fibers**



**Figure 10: Scanning electron microscopy of NF4 A) SEM image of spunbond fibers, B) SEM image of electrospun fibers**

**TGA (Thermogravimetric Analysis) of Prepared Nanofibres:**

**Figure 11: TGA Thermograms of A) NF1 B) NF2 C) NF3 D) NF4**

Thermo gravimetric Analysis (TGA) is pivotal for understanding materials' thermal behavior and stability. Figure No.11 displays TGA thermograms of samples NF1, NF2, NF3, and NF4, revealing their decomposition patterns. TGA subjects samples to controlled temperature ramps, monitoring weight changes. Initial thermograms portions show moisture or volatile components, followed by significant weight loss during main decomposition. Onset and peak temperatures of decomposition offer insights into thermal stability and composition. Thermograms may also indicate residue formation, reflecting sample purity or inorganic filler presence.

## OPTIMIZATION OF PEO (POLYETHYLENE OXIDE) LOADED IN-SITU NANOFIBER GEL:

### Characterization of PEO (Polyethylene Oxide) Loaded In-Situ Nanofiber Gel

#### Determination of pH

NGB3, as the optimized batch, has a pH that is generally acceptable for nasal applications. However, the suitability of each formulation for nasal application also depends on other factors, such as the nature of the active ingredient, formulation stability, and specific requirements of the nasal delivery system.

**Table 8: Determination of pH of Nanofibrous gel**

Sr. No	Formulation Code	pH
1.	NGB1	6.6±0.020
2.	NGB2	6.0±0.010
3.	NGB3	6.3±0.231
4.	NGB 4	6.5±0.452
5.	NGB5	6.3±0.314
6.	NGB6	6.5±0.050
7.	NGB7	6.8±0.040
8.	NGB8	6.6±0.020
9.	NGB9	6.5±0.123
10.	NGB10	6.7±0.010
11.	NGB11	6.9±0.050
12.	NGB12	6.0±0.050

13.	NGB13	6.4±0.030
14.	NGB14	7.2±0.005
15.	NGB15	6.3±0.213

Values are expressed as Mean±S.D.

### ANOVA for Quadratic model

#### Response 1: pH

Source	Sum of Squares	df	Mean Square	F-value	p-value	
<b>Model</b>	1.29	9	0.1434	5.04	0.0448	significant
A-PEO+Sodium alginate	0.3471	1	0.3471	12.21	0.0174	
B-PEO+Chitosan	0.1246	1	0.1246	4.38	0.0905	
C-sodium carboxymethyl cellulose	0.1091	1	0.1091	3.84	0.1075	
AB	0.1800	1	0.1800	6.33	0.0534	
AC	0.0800	1	0.0800	2.81	0.1543	
BC	0.0450	1	0.0450	1.58	0.2639	
A <sup>2</sup>	0.3802	1	0.3802	13.37	0.0146	
B <sup>2</sup>	0.0722	1	0.0722	2.54	0.1719	
C <sup>2</sup>	0.1424	1	0.1424	5.01	0.0754	
<b>Residual</b>	0.1421	5	0.0284			
<b>Cor Total</b>	1.43	14				

Factor coding is **coded**.

Sum of squares is **Type III - Partial**

The **Model F-value** of 5.04 implies the model is significant. There is only a 4.48% chance that an F-value this large could occur due to noise.

**P-values** less than 0.0500 indicate model terms are significant. In this case A, A<sup>2</sup> are significant model terms. Values greater than 0.1000 indicate the model terms are not significant. If there are many insignificant model terms (not counting those required to support hierarchy), model reduction may improve your model.

### Fit Statistics

<b>Std. Dev.</b>	0.1686	<b>R<sup>2</sup></b>	0.9008
<b>Mean</b>	6.50	<b>Adjusted R<sup>2</sup></b>	0.7221
<b>C.V. %</b>	2.59	<b>Predicted R<sup>2</sup></b>	-6.4523
		<b>Adeq Precision</b>	7.1372

A negative **Predicted R<sup>2</sup>** implies that the overall mean may be a better predictor of your response than the current model. In some cases, a higher order model may also predict better.

**Adeq Precision** measures the signal to noise ratio. A ratio greater than 4 is desirable. Your ratio of 7.137 indicates an adequate signal. This model can be used to navigate the design space.

### Final Equation in Terms of Coded Factors

pH	=
+6.04	
-0.1594	A

-0.0955	B
-0.0894	C
+0.1500	AB
-0.1000	AC
+0.0750	BC
+0.2506	A <sup>2</sup>
+0.1092	B <sup>2</sup>
+0.1534	C <sup>2</sup>

The equation in terms of coded factors can be used to make predictions about the response for given levels of each factor. By default, the high levels of the factors are coded as +1 and the low levels are coded as -1. The coded equation is useful for identifying the relative impact of the factors by comparing the factor coefficients.

### Final Equation in Terms of Actual Factors

pH	=
+12.81314	
-1.81320	PEO+Sodium alginate
-1.42577	PEO+Chitosan
-9.34776	sodium carboxymethyl cellulose
+0.150000	PEO+Sodium alginate * PEO+Chitosan
-1.000000	PEO+Sodium alginate * sodium carboxymethyl cellulose
+0.750000	PEO+Chitosan * sodium carboxymethyl cellulose
+0.250629	PEO+Sodium alginate <sup>2</sup>
+0.109208	PEO+Chitosan <sup>2</sup>
+15.34019	sodium carboxymethyl cellulose <sup>2</sup>

The equation in terms of actual factors can be used to make predictions about the response for given levels of each factor. Here, the levels should be specified in the original units for each factor. This equation should not be used to determine the relative impact of each factor because the coefficients are scaled to accommodate the units of each factor and the intercept is not at the center of the design space.

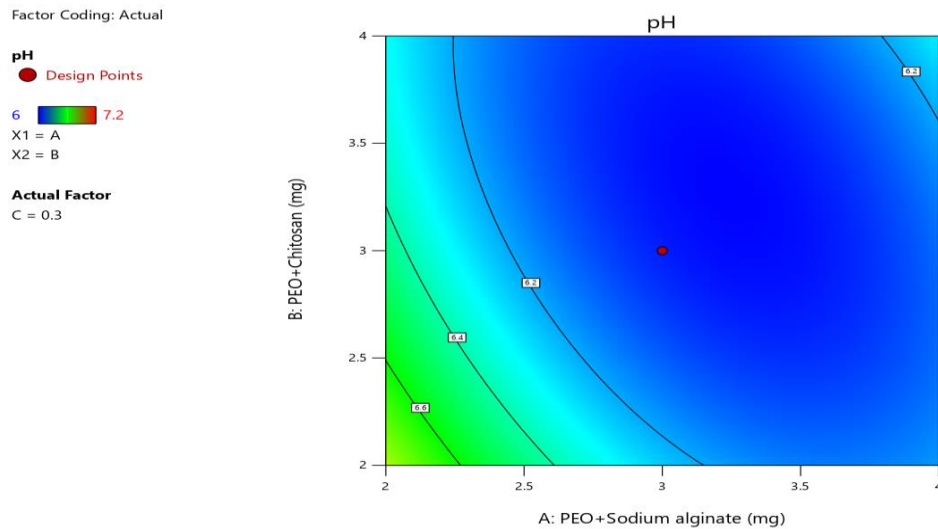


**Figure 11: 2D Counter Plot of pH for (PEO Loaded) Nanofibrous Gel**

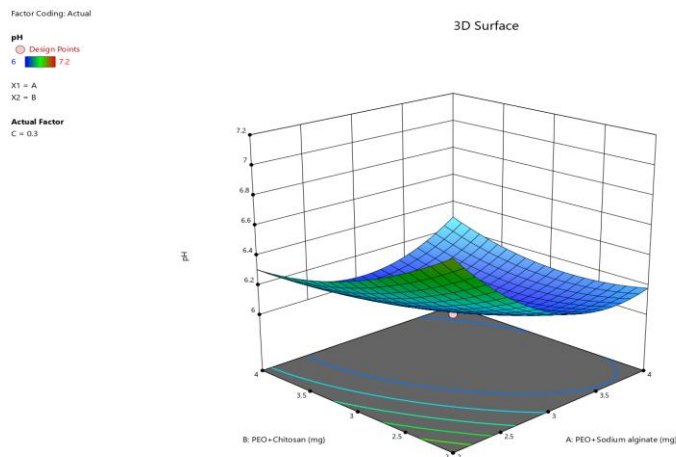


**Figure 12: 3D Response Curve of pH for (PEO Loaded) Nanofibrous Gel.**

### Determination of Viscosity

The optimization of NG 3 as a nasal formulation, characterized by its notably high viscosity of  $445.49 \pm 0.01$  Cps, underscores its potential for targeted objectives within nasal drug delivery. The precision of viscosity measurement, indicated by the relatively low standard deviation, suggests a refined formulation process. This heightened viscosity level may signify tailored attributes such as enhanced drug retention or superior performance within the nasal cavity. As the optimal formulation among those assessed, NG 3 with its viscosity of  $445.49 \pm 0.01$  Cps warrants further investigation to delineate its implications on drug release kinetics, formulation stability, and overall therapeutic efficacy.

**Table 9: Rheological study of Nano fibrous gel**

Sr. No.	Formulation Code	Viscosity (Cps)
1.	NGB1	$170.15 \pm 0.020$
2.	NGB2	$194.74 \pm 0.010$
3.	NGB3	$445.49 \pm 0.010$
4.	NGB 4	$224.50 \pm 1.740$
5.	NGB5	$118.44 \pm 0.020$
6.	NGB6	$219.44 \pm 0.020$
7.	NGB7	$301.28 \pm 0.030$
8.	NGB8	$320.78 \pm 0.025$
9.	NGB9	$325.68 \pm 0.020$
10.	NGB10	$248.53 \pm 0.015$
11.	NGB11	$280.22 \pm 0.020$
12.	NGB12	$218.37 \pm 0.015$
13.	NGB13	$205.08 \pm 0.010$
14.	NGB14	$325.14 \pm 0.025$
15.	NGB15	$315.17 \pm 0.020$

Values are expressed as Mean $\pm$ S.D.

### Determination of Spreadability

The listed formulations ranging from NGB1 to NGB15, the spreadability values vary, with NGB3 emerging as the optimized batch with the highest spreadability at 22 units. Spreadability, indicative of a substance's ability to evenly distribute and cover a surface, plays a crucial role in various applications such as cosmetics, pharmaceuticals, and coatings. While NGB3 stands out with its superior spreadability, other formulations exhibit values ranging from 11.95 to 21.25, each potentially suitable for different contexts depending on specific requirements. The optimization process likely involved a comprehensive evaluation of various factors beyond spreadability alone, ensuring NGB3 meets the desired criteria for its intended use, demonstrating the importance of meticulous formulation and testing in product development.

**Table 10: Spreadability study of Nano fibrous gel**

Sr. No.	Formulation Code	Spreadability (g .cm / sec.)
1.	NGB1	13.70±0.010
2.	NGB2	17.85±0.020
3.	NGB3	11.95±0.120
4.	NGB 4	22.00±0.005
5.	NGB5	21.29±0.030
6.	NGB6	14.99±0.241
7.	NGB7	19.50±0.012
8.	NGB8	12.99±0.314
9.	NGB9	15.40±0.510
10.	NGB10	15.12±0.030
11.	NGB11	18.58±0.020
12.	NGB12	14.36±0.134
13.	NGB13	16.56±0.040

14.	NGB14	22.32±0.050
15.	NGB15	19.94±0.140

Values are expressed as Mean±S.D.

### ANOVA for Linear model

#### Response 2: Spreadability

Source	Sum of Squares	df	Mean Square	F-value	p-value	
<b>Model</b>	87.61	3	29.20	4.47	0.0276	significant
A-PEO+Sodium alginate	77.67	1	77.67	11.90	0.0054	
B-PEO+Chitosan	7.83	1	7.83	1.20	0.2970	
C-sodium carboxymethyl cellulose	2.12	1	2.12	0.3247	0.5802	
<b>Residual</b>	71.82	11	6.53			
<b>Cor Total</b>	159.43	14				

Factor coding is **coded**.

Sum of squares is **Type III - Partial**

The **Model F-value** of 4.47 implies the model is significant. There is only a 2.76% chance that an F-value this large could occur due to noise.

**P-values** less than 0.0500 indicate model terms are significant. In this case A is a significant model term. Values greater than 0.1000 indicate the model terms are not significant. If there are many insignificant model terms (not counting those required to support hierarchy), model reduction may improve your model.

**Fit Statistics**

<b>Std. Dev.</b>	2.56	<b>R<sup>2</sup></b>	0.5495
<b>Mean</b>	17.10	<b>Adjusted R<sup>2</sup></b>	0.4267
<b>C.V. %</b>	14.94	<b>Predicted R<sup>2</sup></b>	0.1340
		<b>Adeq Precision</b>	6.0791

The **Predicted R<sup>2</sup>** of 0.1340 is not as close to the **Adjusted R<sup>2</sup>** of 0.4267 as one might normally expect; i.e. the difference is more than 0.2. This may indicate a large block effect or a possible problem with your model and/or data. Things to consider are model reduction, response transformation, outliers, etc. All empirical models should be tested by doing confirmation runs.

**Adeq Precision** measures the signal to noise ratio. A ratio greater than 4 is desirable. Your ratio of 6.079 indicates an adequate signal. This model can be used to navigate the design space.

**Final Equation in Terms of Coded Factors**

Spreadability	=
+17.10	
-2.38	A
+0.7570	B
+0.3940	C

The equation in terms of coded factors can be used to make predictions about the response for given levels of each factor. By default, the high levels of the factors are coded as +1 and the low levels are coded as -1. The coded equation is useful for identifying the relative impact of the factors by comparing the factor coefficients.

**Final Equation in Terms of Actual Factors**

Spreadability	=
+20.80451	

-2.38474	PEO+Sodium alginate
+0.757016	PEO+Chitosan
+3.93995	sodium carboxymethyl cellulose

The equation in terms of actual factors can be used to make predictions about the response for given levels of each factor. Here, the levels should be specified in the original units for each factor. This equation should not be used to determine the relative impact of each factor because the coefficients are scaled to accommodate the units of each factor and the intercept is not at the center of the design space.

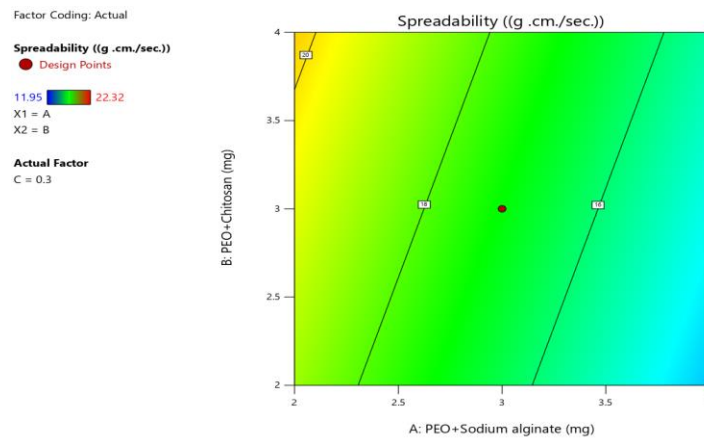


**Figure 13: 2D Counter Plot of Spreadability for (PEO Loaded) Nanofibrous Gel**

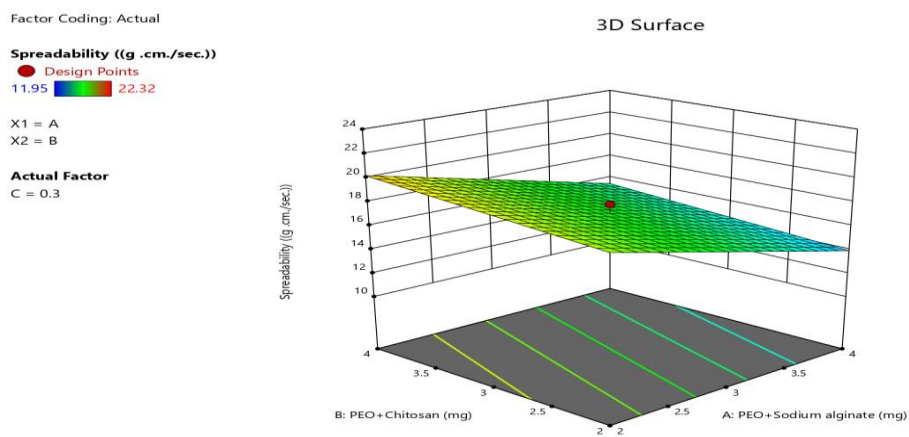


**Figure 14: 3D Response Curve of Spreadability for (PEO Loaded) Nanofibrous Gel**

## Nanofibrous Gel

### Extrudability

NGB3 emerges as the optimal choice due to its superior extrudability, recording the highest value of 22.15 gm. /cm<sup>2</sup>. This indicates NGB3's remarkable ease of dispensing from the collapsible tube, offering practical advantages in terms of user experience and product usability. With its enhanced extrudability, NGB3 presents itself as a promising formulation, ensuring smoother application and potentially enhancing customer satisfaction.

**Table 11: Determination of Extrudability of Nano fibrous gel**

Sr. No.	Formulation Code	Extrudability (gm /cm <sup>2</sup> ).
1	NGB1	16.89±0.140
2	NGB2	13.56±0.020
3	NGB3	22.15±0.214
4	NGB 4	11.23±0.145
5	NGB5	12.54±0.050
6	NGB6	14.67±0.040
7	NGB7	13.89±0.030
8	NGB8	17.88±0.010
9	NGB9	18.99±0.020
10	NGB10	16.87±0.050
11	NGB11	17.46±0.231
12	NGB12	12.36±0.120

<b>13</b>	NGB13	13.25±0.050
<b>14</b>	NGB14	14.89±0.020
<b>15</b>	NGB15	16.45±0.040

Values are expressed as Mean±S.D.

### Drug Content Uniformity

The drug content of a dosage form is crucial for its efficacy and uniformity. NGB3, the optimized batch, has the highest drug content at 96.89±0.01%, indicating its potential effectiveness. However, variability exists across formulations like NGB5, NGB6, and NGB14, emphasizing the need for consistent drug content to ensure the system's efficacy and uniformity.

**Table 12: Determination of drug content of PEO Loaded Nano fibrous gel**

<b>Sr. No.</b>	<b>Formulation Code</b>	<b>Drug Content (%)</b>
1	NGB1	80.15±0.625
2	NGB2	95.16±0.015
<b>3</b>	<b>NGB3</b>	<b>96.89±0.010</b>
4	NGB 4	95.19±0.021
5	NGB5	90.00±1.000
6	NGB6	86.00±1.528
7	NGB7	89.99±0.010
8	NGB8	85.00±0.577
9	NGB9	86.87±0.005
10	NGB10	79.46±0.010

11	NGB11	84.00±0.577
12	NGB12	82.58±0.021
13	NGB13	86.40±0.100
14	NGB14	91.00±1.055
15	NGB15	81.15±0.090

Values are expressed as Mean±S.D. (n=3)

### In vitro drug diffusion study

The in vitro release profile study was carried out using Franz diffusion cell concludes the amount of drug release from the gel on the skin from nanogel dispersion on was found to be from in situ nanogel dispersion was found to be maximum 94.15% for formulation NG3up to 12 hr.

**Table 13: Drug release profile of gel**

<b>Formulation Code / Time in Hrs.</b>	<b>0.5</b>	<b>1</b>	<b>2</b>	<b>4</b>	<b>8</b>	<b>12</b>
NGB1	32.17±0.010	35.86±0.015	49.78±0.026	64.55±0.021	75.51±0.040	88.59±0.010
NGB2	30.83±0.010	45.33±0.190	50.33±0.025	69.55±0.011	72.54±0.010	80.77±0.020
<b>NGB3</b>	<b>38.92±0.015</b>	<b>49.14±0.020</b>	<b>60.03±0.020</b>	<b>72.66±0.010</b>	<b>84.45±0.010</b>	<b>94.15±0.023</b>
NGB 4	33.49±0.015	49.43±0.005	60.15±0.010	62.88±0.010	71.88±0.010	87.55±0.023
NGB5	36.56±0.047	48.99±0.020	65.46±0.032	77.94±0.020	86.57±0.015	90.75±0.020

NGB6	32.12±0.030	42.99±0.274	55.59±0.025	60.47±0.010	73.64±0.030	80.45±0.020
NGB7	24.59±0.020	30.49±0.020	45.16±0.015	58.44±0.011	68.66±0.036	75.88±0.015
NGB8	28.47±0.015	39.47±0.010	44.12±0.020	57.4±0.152	67.18±0.020	82.26±0.030
NGB9	36.49±0.020	49.89±0.015	52.16±0.020	59.54±0.010	71.48±0.030	83.59±0.020
NGB10	25.49±0.150	39.77±0.011	55.4±0.251	62.77±0.015	70.36±0.035	78.69±0.020
NGB11	35.4±0.200	42.77±0.005	55.76±0.015	67.14±0.010	72.3±0.173	79.89±0.011
NGB12	58.46±0.015	59.99±0.216	64.89±0.010	68.74±0.001	70.02±0.007	71.35±0.010
NGB13	30.74±0.010	42.77±0.015	54.55±0.015	65.66±0.001	78.45±0.005	85.69±0.015
NGB14	31.58±0.005	43.16±0.02	57.64±0.010	76.77±0.015	82.15±0.020	88.47±0.011
NGB15	27.47±0.010	39.56±0.01	48.49±0.015	52.47±0.015	75.47±0.010	89.75±0.010

Values expressed as Mean ± S.D.

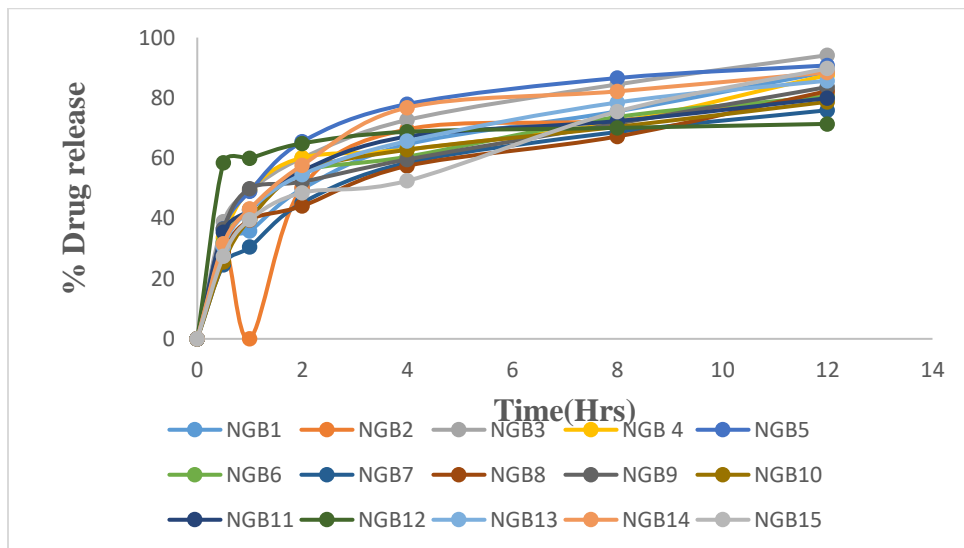


**Figure 15: Percent (%) Drug Release of All Optimized Batches of (PEO Loaded) Nanofibrous Gel**

**Kinetic analysis of drug release-**

In order to define the release mechanism that gives the best description of the release pattern; the in vitro release data for all optimized batches were fitted to kinetic equations models. The kinetic equations were used i.e., zero, first-order and Higuchi model. Both the kinetic rate constant (k) and the determination coefficient (R2) were calculated and presented in below graphs. The best fit model with the highest determination coefficient (R2) value for optimized batch was Higuchi model.

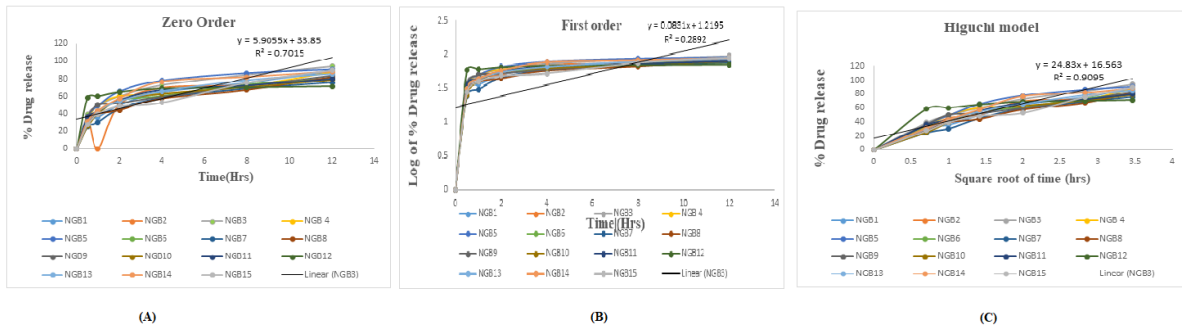


**Figure 16: (A) Zero order of optimized batches, (B) First order of optimized batches, (C) Higuchi model of optimized batches**

**Table 14: R2 value of kinetic models**

Models	Optimized Batches	R2 Value
Zero order	NGB3	0.7015
First order	NGB3	0.2892
Higuchi model	NGB3	0.9095

### In-vivo activity

#### Streptozotocin induced antidiabetic activity

In vivo anti-diabetic study was performed for formulated PEO Loaded Nanogels.

The blood glucose levels are tabulated in Table: 15.

**Table 15: Initial and final blood glucose level before and after streptozotocin administration PEO Loaded nanofibrous gel.**

GROUPS	Glucose Level on Day 0 (mg/dl)	Glucose Level on Day 7 (mg/dl)	Glucose Level on Day 14 (mg/dl)	Glucose Level on Day 28 (mg/dl)
Positive Control	124.23±3.68	128.56±4.38	138.58±2.56	132.47±1.96
Disease Inducer Control	129.24±3.45 <sup>ns</sup>	227.29±4.28 <sup>@</sup>	242.78±5.68 <sup>@</sup>	236.24±2.75 <sup>@</sup>
Metformin Standard	122.39±6.15 <sup>ns</sup>	236.19±3.21 <sup>ns</sup>	162.69±3.64 <sup>**</sup>	129.53±4.93 <sup>**</sup>

Nanogel NGB-3	132.36±4.19 <sup>ns</sup>	231.89±3.56 <sup>**</sup>	163.85±6.32 <sup>**</sup>	148.31±3.58 <sup>**</sup>
---------------	---------------------------	---------------------------	---------------------------	---------------------------

The results were expressed as mean SD (n = 6),

ns p>0.05, non-significant; \*\*p<0.01, very significant; when compared to Negative Control group. @ p<0.01, when compared with Positive control group

Based on the provided data on glucose levels over the course of the experiment, here is a conclusion drawn regarding the anti-diabetic activity:

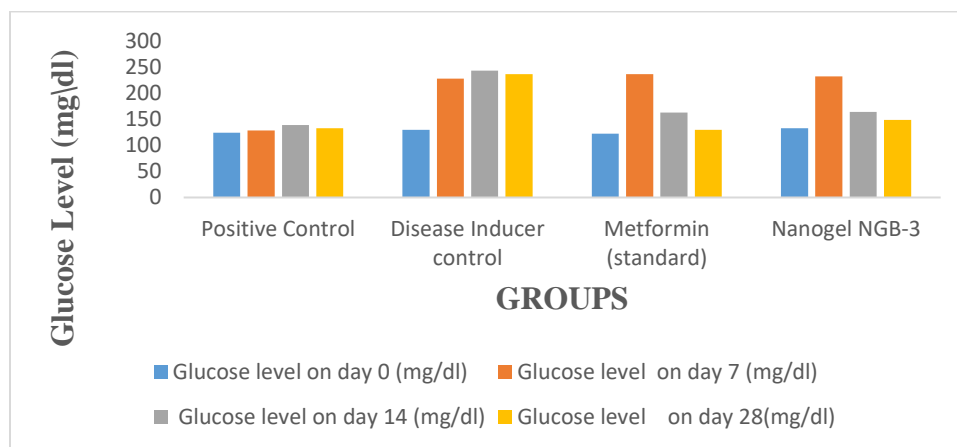


**Figure: Initial and Final Blood Glucose Level Before and After Streptozotocin Administration PEO Loaded Nanofibre Gel.**

#### Stability study of PEO loaded Nano fibrous gel:

The NGB3 nasal formulation demonstrates good stability in terms of spreadability, viscosity, and drug content over a three-month storage period. The small variations observed in these parameters are within an acceptable range for pharmaceutical formulations, suggesting that NGB3 has the potential for extended shelf life without significant changes in critical quality attributes. However, continued monitoring is advisable for longer-term storage to ensure sustained stability.

**Table 17: Stability study of Nano fibrous gel (PEO)**

Storage Duration	Formulation Code	Spreadability (g .cm /sec.)	Viscosity(Cp)	Drug Content (%)
“0” Month	NGB3	11.95±0.120	445.49±0.010	96.89±0.010

<b>“1” Month</b>	<b>NGB3</b>	11.95±0.005	445.49±0.001	96.89±0.001
<b>“2” Month</b>	<b>NGB3</b>	11.94±0.150	445.48±0.001	96.85±0.011
<b>“3” Month</b>	<b>NGB3</b>	11.93±0.010	445.48±0.001	96.85±0.07

Values expressed as Mean ± S.D.

### CONCLUSION:

Nanofiber formulations loaded with Bovine Insulin were prepared using electrospinning. The Bovine Insulin-loaded nanofibers were optimized and then incorporated into an in-situ nasal gel. Preformulation studies included HPLC validation of Bovine Insulin and compatibility studies using FTIR, DSC, and XRD. Thiol groups were quantified for chitosan and sodium alginate conjugates. Characterization of nanofibers included evaluation of drug entrapment efficiency, swelling index, and SEM analysis. PEO-loaded in-situ nanofiber gels were optimized for pH, viscosity, spreadability, and extrudability using ANOVA. The optimized formulation showed suitable characteristics for nasal application. Antidiabetic efficacy of the optimized NB3 batch was evaluated through in vivo studies, likely using diabetic animal models.

### CONFLICT OF INTEREST:

The authors declare no conflict of interest.

### REFERENCE

1. Gopal R, Kaur S, Ma Z, Chan C, Ramakrishna S, Matsuura T. Electrospun nanofibrous filtration membrane. *Journal of Membrane Science*. 2006 Sep 15;281(1-2):581-6.
2. Kowalczyk T, Nowicka A, Elbaum D, Kowalewski TA. Electrospinning of bovine serum albumin. Optimization and the use for production of biosensors. *Biomacromolecules*. 2008 Jul 14;9(7):2087-90.
3. Lu T, Chen X, Shi Q, Wang Y, Zhang P, Jing X. The immobilization of proteins on biodegradable fibers via biotin–streptavidin bridges. *Acta Biomaterialia*. 2008 Nov 1;4(6):1770-7.
4. Pillay V, Dott C, Choonara YE, Tyagi C, Tomar L, Kumar P, du Toit LC, Ndesendo VM. A review of the effect of processing variables on the fabrication of electrospun nanofibers for drug delivery applications. *Journal of Nanomaterials*. 2013 Dec;2013.

5. Xue J, Wu T, Dai Y, Xia Y. Electrospinning and electrospun nanofibers: Methods, materials, and applications. *Chemical reviews*. 2019 Mar 27;119(8):5298-415.
6. Ahmed FE, Lalia BS, Hashaikeh R. A review on electrospinning for membrane fabrication: Challenges and applications. *Desalination*. 2015 Jan 15;356:15-30.
7. Abdulhussain R, Adebisi A, Conway BR, Asare-Addo K. Electrospun nanofibers: Exploring process parameters, polymer selection, and recent applications in pharmaceuticals and drug delivery. *Journal of Drug Delivery Science and Technology*. 2023 Nov 10:105156.
8. Kaur P, Garg T, Rath G, Goyal AK. In situ nasal gel drug delivery: A novel approach for brain targeting through the mucosal membrane. *Artificial cells, nanomedicine, and biotechnology*. 2016 May 18;44(4):1167-76.
9. Al-Naamani L, Dobretsov S, Dutta J, Burgess JG. Chitosan-zinc oxide nanocomposite coatings for the prevention of marine biofouling. *Chemosphere*. 2017 Feb 1;168:408-17.
10. Augustine R, Rehman SR, Ahmed R, Zahid AA, Sharifi M, Falahati M, Hasan A. Electrospun chitosan membranes containing bioactive and therapeutic agents for enhanced wound healing. *International journal of biological macromolecules*. 2020 Aug 1;156:153-70.
11. Cardenas Bates II, Loranger É, Chabot B. Chitosan-PEO nanofiber mats for copper removal in aqueous solution using a new versatile electrospinning collector. *SN Applied Sciences*. 2020 Sep;2(9):1540.
12. Ahmed A, Xu L, Yin J, Wang M, Khan F, Ali M. High-throughput fabrication of chitosan/poly (ethylene oxide) nanofibers by modified free surface electrospinning. *Fibers and Polymers*. 2020 Sep;21:1945-55.
13. Saatchi A, Arani AR, Moghanian A, Mozafari M. Synthesis and characterization of electrospun cerium-doped bioactive glass/chitosan/polyethylene oxide composite scaffolds for tissue engineering applications. *Ceramics International*. 2021 Jan 1;47(1):260-71.
14. Amiri N, Ajami S, Shahroodi A, Jannatabadi N, Darban SA, Bazzaz BS, Pishavar E, Kalalinia F, Movaffagh J. Teicoplanin-loaded chitosan-PEO nanofibers for local antibiotic delivery and wound healing. *International Journal of Biological Macromolecules*. 2020 Nov 1;162:645-56.

15. Satheeshababu BK, Shruthinag R. Synthesis and charactersiation of chitosan conjugate; design and evaluation of membrane moderated type transdermal drug delivery system. Indian journal of pharmaceutical sciences. 2015 Jul;77(4):405.
16. Jindal AB, Wasnik MN, Nair HA. Synthesis of thiolated alginate and evaluation of mucoadhesiveness, cytotoxicity and release retardant properties. Indian Journal of Pharmaceutical Sciences. 2010 Nov;72(6):766.
17. Kurniawan DW, Fudholi A, Susidarti RA. Synthesis of thiolated chitosan as matrix for the preparation of metformin hydrochloride microparticles. Research in Pharmacy. 2015 Oct 29;2(1).
18. Park JC, Ito T, Kim KO, Kim KW, Kim BS, Khil MS, Kim HY, Kim IS. Electrospun poly (vinyl alcohol) nanofibers: effects of degree of hydrolysis and enhanced water stability. Polymer journal. 2010 Mar; 42(3):273-6.
19. Bayuo J, Abukari MA, Pelig-Ba KB. Optimization using central composite design (CCD) of response surface methodology (RSM) for biosorption of hexavalent chromium from aqueous media. Applied Water Science. 2020 Jun;10(6):1-2.
20. Bayuo J, Abukari MA, Pelig-Ba KB. Optimization using central composite design (CCD) of response surface methodology (RSM) for biosorption of hexavalent chromium from aqueous media. Applied Water Science. 2020 Jun;10(6):1-2.
21. Aruna M, Gandhimathi R. Formulation and Evaluation of Ganciclovir Niosomes by Box–Behnken Experiment Design. LATIN AMERICAN JOURNAL OF PHARMACY. 2023 Jan 1;42(1):169-78.
22. Ahmadi S, Akbarzadeh I, Chiani M, Seraj M, Noorbazargan H, Saffar S, Quazi S, Far BF. An Optimized and Well-characterized Niosome-based Nanocarrier for Letrozole: A Brand-new Hybrid Therapy for Breast Cancer.
23. Bahmani S, Khajavi R, Ehsani M, Rahimi MK, Kalae MR. Transdermal drug delivery system of lidocaine hydrochloride based on dissolving gelatin/sodium carboxymethylcellulose microneedles. AAPS Open. 2023 Apr 3;9(1):7.
24. Neha A, Himanshi K, Deepa P, Nageen A, Tarun G. Evaluation of entrapment efficiency of glipizide microsphere. IOSR Journal of pharmacy. 2012 Mar;2(2):180-81.

25. Çay A, Miraftab M, Kumbasar EP. Characterization and swelling performance of physically stabilized electrospun poly (vinyl alcohol)/chitosan nanofibres. *European polymer journal*. 2014 Dec 1;61:253-62.
26. Jacob S, Nair AB, Al-Dhubiab BE. Preparation and evaluation of niosome gel containing acyclovir for enhanced dermal deposition. *Journal of liposome research*. 2017 Oct 2;27(4):283-92.
27. Stan CD, Tataringa G, Gafitanu C, Dragan M, Braha S, Popescu MC, Lisa G, Stefanache A. Preparation and characterization of niosomes containing metronidazole. *Farmacia*. 2013 Nov 1;61(6):1178-85.
28. Aiyalu R, Govindarjan A, Ramasamy A. Formulation and evaluation of topical herbal gel for the treatment of arthritis in animal model. *Brazilian Journal of Pharmaceutical Sciences*. 2016 Jul;52:493-507.
29. Choudhary V, Rani D, Ghosh N, Kaushik M. DEVELOPMENT AND EVALUATION OF HYDROCORTISONE-LOADED NIOSOMAL GEL.
30. Suresh RV, Kerunath KP. Formulation and evaluation of novel anti-bacterial ciprofloxacin loaded niosomal cream. *Int. Res. J. Pharm*. 2015;6(8):519-27.
31. Inamdar YM, Rane B, Jain A. Preparation and evaluation of beta sitosterol nanogel: A carrier design for targeted drug delivery system. *Asian Journal of Pharmaceutical Research and Development*. 2018 Aug 3;6(3):81-7.
32. Rane S, Inamdar Y, Rane B, Ashish J. Niosomes: a non-ionic surfactant based vesicles as a carriers for drug delivery. *International Journal of Pharmaceutical Sciences Review and Research*. 2018 Jul;51(1):198-213.
33. Gujarathi NA, Patil TS, Rane BR, Babu A, Keservani RK. Micro-and Nano-Systems in Transdermal Drug Delivery. In *Topical and Transdermal Drug Delivery Systems 2023* Feb 6 (pp. 41-78). Apple Academic Press.
34. Gujarathi NA, Patil TS, Rane BR, Babu A, Keservani RK. Micro-and Nano-Systems in Transdermal Drug Delivery. In *Topical and Transdermal Drug Delivery Systems 2023* Feb 6 (pp. 41-78). Apple Academic Press.
35. Zhou T, Xu X, Du M, Zhao T, Wang J. A preclinical overview of metformin for the treatment of type 2 diabetes. *Biomedicine & Pharmacotherapy*. 2018 Oct 1;106:1227-35.

36. Satyanarayana N, Chinni SV, Gobinath R, Sunitha P, Uma Sankar A, Muthuvenkatachalam BS. Antidiabetic activity of Solanum torvum fruit extract in streptozotocin-induced diabetic rats. *Frontiers in nutrition*. 2022 Oct 28;9:987552.
37. Iqbal MK, Iqbal A, Anjum H, Gupta MM, Ali J, Baboota S. Determination of in vivo virtue of dermal targeted combinatorial lipid nanocolloidal based formulation of 5-fluorouracil and resveratrol against skin cancer. *International Journal of Pharmaceutics*. 2021 Dec 15;610:121179.